J. Min. Metall. Sect. B-Metall. 61 (3) (2025) 345 - 355

Journal of Mining and Metallurgy, Section B: Metallurgy

THE INFLUENCE OF Cu CONTENT ON THE MICROSTRUCTURE AND MECHANICAL PROPERTIES OF PM-FABRICATED Ti-18Nb-XCu ALLOY

Huseyin Demirtas [a,*], Rana Afif Anaee [b], Muhamad Saad Faaik [a]

[a] Karabuk University, Machinery and Metal Technologies Department, Karabuk, Turkiye
[b] University of Technology, Materials Engineering Department, Baghdad, Iraq

(Received 22 September 2024; Accepted 26 November 2025)

Abstract

This research investigated the influence of varying copper (Cu) concentrations (0, 5, 7, and 9 wt.%) on the sintering behaviour, microstructural development, and mechanical characteristics of Ti-18Nb alloy, fabricated through conventional powder metallurgy. Under specific sintering conditions (1150°C for 5 hours), Cu addition led to a more homogeneous microstructure and promoted the complete dissolution of Nb particles. X-ray diffraction (XRD) analysis confirmed the presence of alpha (α) and beta (β) Ti phases, along with the Ti_2Cu phase, with its peak intensity increasing as Cu content rose. Mechanical properties were significantly enhanced by Cu addition. Yield strength increased almost linearly with Cu content. Compressive strength notably increased with 7 wt.% Cu, reaching 980 MPa, and slightly exceeded this value with 9 wt.% Cu. Hardness values increased due to solid solution strengthening in the α-Ti phase and the precipitation of the Ti_2Cu phase, with the highest hardness (222 HV) observed in the 7 wt.% Cu alloy. The elastic modulus initially increased with 5 wt.% Cu, then subsequently decreased with further Cu additions; the Ti-18Nb-7Cu alloy exhibited the lowest elastic modulus at 13.34 GPa. Furthermore, the resilience of the alloys improved with the formation of the Ti_2Cu phase, and a maximum value of 13.15 MJ m^{-3} was achieved.

Keywords: *Ti alloy; Biomaterial; Powder metallurgy; Compression test; Elastic modulus; Resilience*

1. Introduction

Pure titanium (Ti) and Ti-6Al-4V (TAV) are the most commonly used biomedical materials among Ti-based alloys [1]. However, the mechanical properties of Ti as an implant material do not fully meet the requirements. The addition of vanadium (V) and aluminium (Al) improves their mechanical properties but significantly degrades their biological properties due to the negative effects of Al and the toxicity of V [2, 3]. Consequently, many studies have focused on beta (β) and near β phase titanium-based alloys with non-toxic alloying elements such as Nb, Mo, Zr, Ta, and Sn. These alloys have several advantages for orthopaedic implants, in particular, better biocompatibility and bio-corrosion resistance [4–6].

In newly developed biocompatible alloys, niobium (Nb) is highlighted as an alternative to the harmful beta stabilizer (V). It also exhibits β-stabilizing properties and is non-allergenic and non-toxic [7, 8]. Moreover, shape memory (SM) properties of Ti-Nb alloys have been extensively studied [9–11]. SM and superelasticity (SE) properties have also been investigated for Ti-V and Ti-Mo alloys [12, 13]. However, Ti-V alloys are unsuitable for biomaterial applications because of the cytotoxicity of V, and Ti-Mo alloys are sensitive to ω phase embrittlement [14]. Hence, Ti-Nb alloys are more suitable for biomedical applications with various advantages besides high corrosion resistance and low elastic modulus.

The elastic modulus of metal implants significantly affects successful implantation, as natural bone resorption and implant loosening may occur due to stress shielding [2, 15]. However, human cortical bone has a much lower elastic modulus (10-30 GPa) than most of the metallic implant materials, such as Ti and some Ti alloys [2, 16]. The modulus of elasticity of TAV alloy, one of the most widely used biomaterials, is 110 GPa [17]. The mechanical properties can be optimised to overcome this disadvantage by controlling the alloying elements and relative densities [18].

Powder metallurgy (PM) is one of the most effective methods for density control [19]. For instance, while the density of Ti–18Nb–4Sn alloy produced by the PM method is 97%, its elastic modulus was determined as 75.8 GPa. However, this

Corresponding author: hdemirtas@karabuk.edu.tr

https://doi.org/10.2298/JMMB240922027D

value ranged from 10.8–33.2 GPa when the relative density was reduced to 0.4–0.7 [20]. A primary function of porosity in orthopaedic metal implants is to support tissue adhesion and growth. Improving the interfacial bond between bone tissue and implant materials can enhance the in vivo life of load-bearing implants. Another function is to control the elasticity modulus and match it to that of bone [21, 22].

Copper (Cu) has been widely used as an alloying element for Ti alloys, due to its remarkable biocompatibility and antibacterial properties [23–26]. It has been proven that Ti-Cu alloys containing more than 5% Cu by weight have high antibacterial activity against E. coli and S. aureus [26]. In addition to antibacterial activity, Cu content can also affect mechanical and corrosion properties [26, 27]. Furthermore, the melting point of Cu (1084 ˚C) is close to the sintering temperature of Ti-Nb alloys, and the liquid phase formed by Cu can positively affect the sintering process [28]. Moreover, the addition of Cu reduces the melting point of the Ti-Cu mixture and facilitates sintering [29]. These changes occurring during the sintering process will also affect the pores formed in the conventional PM method. It is also known that Cu added to Ti in sufficient amounts forms Ti_2Cu precipitates [30].

Numerous studies have been carried out on the effects of Nb addition to Ti, and some of them have demonstrated that Cu addition increases the antibacterial properties of Ti [25, 26]. However, it is not sufficiently clear how Cu addition affects the mechanical performance of Ti-Nb alloys. Moreover, despite the positive effects of porosity on biocompatibility and mechanical properties in biomaterials, studies on alloys produced by the PM method are limited. Another critical issue in the PM method is the effect of Cu addition on sintering. Therefore, this study aims to examine the mechanical properties of Ti-18Nb alloys containing varying amounts of Cu produced by the PM method.

2. Experimental Procedures

To investigate the influence of Cu addition on Ti-Nb alloys, three varying amounts (5, 7 and 9 wt.%) of Cu were added to the base alloy. The addition of Cu was compensated by proportionally decreasing the Ti content. Sample production was carried out by the PM method. The Ti (99.9% purity), Nb (99.8% purity) and dendritic Cu (purity >99.5%) powders used in this study are shown in Fig. 1.

To prepare the samples, the powders were weighed in the indicated ratios and mixed in a Turbula T2F triaxial mixer for one hour. The mixed powders were pressed uniaxially in a cylindrical steel mold with a 13 mm diameter at room temperature (RT) without lubricants or binders. Compression pressures of 450 MPa, 500 MPa and 600 MPa were evaluated, and 500 MPa was selected based on optimum results. To reduce potential density gradients arising from single-sided pressure application in relatively tall compacts, incremental powder loading, manual tapping, and a slow pressing rate were carefully employed to ensure uniform stress distribution and minimize friction-induced inhomogeneity.

After vacuuming, green samples were sintered in a cylindrical tube furnace (Protherm PZF) under a protective Ar atmosphere. Sintering temperature and time were chosen based on the results from previous studies [18, 27]. The furnace temperature was gradually increased at a rate of 10˚C per minute until it reached 1150˚C. At that temperature, the samples were sintered for a period of 5 hours and then cooled to 150˚C in the furnace. Compression tests and density measurements were performed immediately after sintering. Some samples were cut, and metallurgical surfaces were prepared for microstructure analyses, XRD and hardness measurements.

Densities of sintered samples were determined according to the Archimedes principle. Distilled water

Figure 1. *Image of powders used in sample production*

was used in experiments performed at room temperature and normal pressure. Petroleum jelly was used to prevent water leakage into the sample from the pores formed on the surface. These measurements were performed on at least eight samples for each alloy. Based on these measurements, average density values were determined, and volumetric porosity was calculated as a ratio to the theoretical density.

Compression tests were applied on samples using the Zwick/Roell Z600 universal tension-compression test machine at a strain rate of 0.2 mm/min. After sintering, the samples obtained in approximately Ø13 mm × 25 mm dimensions were checked for surface parallelism and after grinding the required surfaces, compression test specimens were obtained. Tests were performed in accordance with ASTM E 9 – 89a and each alloy was evaluated three times to ensure consistent data.

Hardness measurements were taken as macro and micro scales due to the presence of pores in the samples and the lack of a homogeneous microstructure after sintering in some alloys. Macro hardness (Brinell) was determined using the Qness Q250M instrument, applying a 62.5 kg load for 10 seconds with a 2.5 mm steel ball indenter. Microhardness (Vickers) was measured using the QNESS Q10 A+ device with a 1 kg load applied for 15 seconds. To ensure accuracy and reliability, average hardness values were obtained from at least five measurements.

For microstructure analysis, the cut samples were ground using SiC paper of grain sizes ranging from 240 to 1200 grit. Subsequently, polishing was performed using 6μm diamond particles. Samples were etched using Kroll's reagent to reveal microstructural details.

For microstructure characterization, Carl Zeiss Ultra Plus Gemini (FESEM) equipped with a Bruker Energy-Dispersive X-ray Spectrometer (EDS) was used. In addition to examining the pore morphology and microstructure, the chemical compositions of the formed phases were determined. Microstructure images were further analysed using the ImageJ software to quantify and evaluate the presence of pores.

XRD measurements were performed using a Rigaku Ultra IV diffractometer to determine the phases present in the alloys. Measurements were conducted with a 2 kW X-Ray Cu tube at a scanning speed of 4 deg/min, and diffraction patterns were obtained between 10 and 90 degrees 2θ (Bragg angles). The performance and sensitivity of XRD are related to the scanning speed and better resolution can be achieved at slower speeds. However, this speed (4 deg/min) was found to be sufficient for the qualitative examination in this study.

3. Results and Discussion

The chemical compositions, measured average densities, and volumetric porosity of the alloys are presented in Table 1. The chemical compositions represent the average actual values measured by EDS. An approximate 18% porosity indicates a potential for further densification of the alloy [31]. For comparison, a Ti–13Nb–13Zr alloy, processed under similar conditions, achieved 98.6% density after sintering at 1250°C for 4 hours with a 360 MPa compression [32]. In another study, hot isostatic pressing (HIP) was applied to Ti-Nb alloys after cold pressing, and 4 vol% porosity was achieved after 1100˚C sintering [33]. However, natural pores were desired, no additional densification process was applied in this study. The modulus of elasticity is a crucial factor in biomaterials, and Gibson and Ashby [34] theoretically proved that the relative density influences the elastic modulus.

Porosity decreased with the addition of 5 wt.% Cu, compared to the reference material, and then the porosity remained almost constant with the increasing amount of Cu. During the sintering process, the Cu phase can exist in two primary states and increase density accordingly. If it is in the alloy, the addition of Cu may increase the efficiency of sintering by lowering the melting point of the Ti-Cu phase [29]. Or the Cu phase may form a liquid phase among other particles with high melting temperature [35]. In addition, in the pressing process, both the shape (dendritic) and mechanical properties of pure Cu powder are expected to affect the compaction of powder mixtures positively.

Table 1. *Composition, density and volumetric porosity of alloys*

Samples	Measured compositions (wt.%)			Measured Density (g/cm^3)	Volumetric Porosity (%)
	Ti	Nb	Cu		
Ti-18Nb	78.4	21.6	-	4.01 ± 0.10	18.58
Ti-18Nb-5Cu	75	20.8	4.2	4.17 ± 0.07	17.48
Ti-18Nb-7Cu	72.1	20.5	7.4	4.22 ± 0.06	17.51
Ti-18Nb-9Cu	73	17.8	9.2	4.27 ± 0.07	17.59

The addition of Cu also affected the phases formed in the microstructure; the formed phases are seen in the XRD analysis given in Fig. 2b. The analysis revealed that the Ti-Nb alloys primarily consisted of alpha (α) and beta (β) Ti phases. In addition, a small amount of undissolved Nb was detected, as observed in the microstructure investigations (Fig. 3). However, since it is difficult to detect small amounts of phases with general XRD analysis and the phase patterns of Nb and β-Ti are almost coincident (2θ values: 38.3˚, 55.3˚, 69.3˚ and 82.1˚), they could not be clearly identified and labelled. It should be noted that minor Al and O signals are detected in the EDS spectra (Fig. 3), likely originating from residual alumina from polishing and/or slight surface oxidation. These signals are localized and minor, and do not significantly affect the chemical composition, phase formation, or mechanical properties of the alloys.

XRD analyses revealed that the Ti_2Cu phase was formed with the addition of 5 wt.% Cu and higher concentrations to the base alloy. With increasing Cu content, the peaks at 43.6˚ and 77.5˚ corresponding to the Ti_2Cu phase (JCPDS No. 14-0641) exhibited a distinct increase in intensity. In a study on the mechanical and tribological properties of Ti-Cu alloys, Xu et al. [30] observed that the amount of Ti_2Cu intermetallic phase increased with increasing Cu concentrations. Despite the variation in Ti_2Cu intensity, all Cu-containing alloys presented a similar set of phases (α, β, and Ti_2Cu). From the Ti-Cu binary phase diagram, it can be deduced that the Ti_2Cu phase can only be formed at Cu compositions less than 40% [29]. The Ti-Nb-Cu triple phase diagram (Fig. 2a) indicates that only α and β-Ti phases form when less than 5 wt.% Cu is added to the Ti-18Nb alloy. However, as the Cu content increases, the Ti_2Cu phase begins to form in addition to these phases, and the amount of these precipitates increases with increasing Cu content. In addition, according to this phase diagram, with the increasing amount of Cu, the structure consists predominantly of β-Ti and Ti_2Cu. This transformation indicates that increasing Cu content promotes β phase formation [29].

The microstructure of all alloys generally consists of α and β-Ti phases (Figs. 5 and 6). However, some Nb-rich regions appear in the Ti-18Nb base alloy. In Fig. 3, the whitish regions correspond to Nb-rich areas that contain almost no Ti, and the light grey areas surrounding these regions contain approximately two-thirds Nb by weight. Although the whitish Nb-rich regions are relatively rare, the light grey areas are scattered throughout the microstructure. In contrast, Fig. 4 presents the low-magnification (100x) microstructures of the Cu-containing alloys, in which no whitish Nb-rich regions are observed. Light grey regions are detected only in limited amounts in the Ti-18Nb-5Cu alloy. These observations provide further evidence that Cu addition enhances the sintering process and promotes the dissolution of Nb particles. Consistent with the Ti-Cu binary phase diagram [36], even the addition of 5 wt.% Cu reduces the melting point of Ti by approximately 20%, and this decrease continues with increasing Cu up to 1005˚C.

β-Ti structure formation begins with the dissolution of Nb particles at about 900˚C and increases proportionally to the amount of dissolved Nb [37]. Ti-10Nb and Ti-15 Nb alloys were sintered from 900˚C to 1500˚C, and Nb-rich phases in both alloys up to 1100˚C were observed [38]. In addition, the shape of these Nb-rich phases was irregular after sintering at 900˚C, and they were spherical after sintering at 1100˚C, as in that study. In another study on this subject, Zhao et al. [39] stated that the sintering temperature should be 1300˚C on average

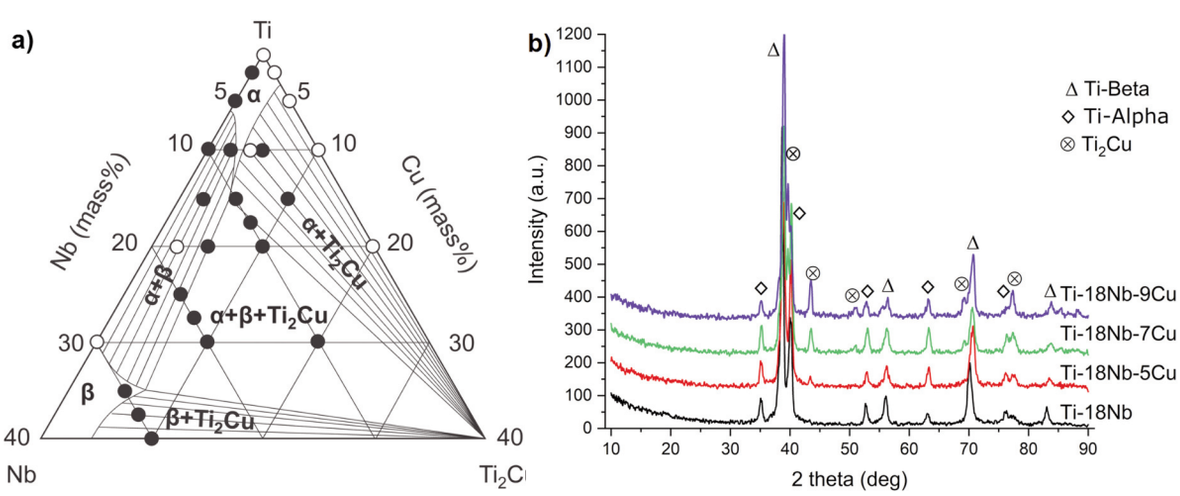

Figure 2. *a) Ti-Nb-Ti_2Cu phase diagram [29] and b) XRD measurements of our alloys*

for complete homogenisation in Ti-Nb alloys. However, Cu was not added in the mentioned studies. In this study, lower sintering temperatures were tried, considering that the addition of Cu would have a positive effect on sintering. As a result, this study showed that the Cu addition supported the formation of a homogeneous microstructure by ensuring the dissolution of Nb during the sintering stage and that 1150˚C was sufficient for 5 wt.% and more Cu-added samples.

The microstructure of Cu-added alloys consists of light-coloured regions and homogeneously distributed lath-like dark phases. Niobium concentration is higher in the light-coloured areas and lower in the darker areas (Fig. 5, line EDS). The light-coloured regions, indicating enrichment in the beta-stabilizer Nb, are identified as β-Ti, while the darker regions are designated as α-Ti. During furnace cooling after sintering, the β-Ti phase decomposed through either α-phase precipitation or a eutectoid transformation. The thick dark grey areas observed in Fig. 5 represent α-Ti phases in the microstructure. No evidence of fine α-phase formation or martensitic transformation was observed at the cooling rate employed in this study. Although the Ti_2Cu phase appeared in XRD analysis (Fig. 2b) of all Cu-added alloys, it was not determined in the microstructures. It has been stated that these precipitates usually occur at the nanoscale in the microstructure [40, 41].

While the Cu-containing alloys generally exhibited similar microstructures, the alloy with 9 wt.% Cu distinctly featured differing, ash-grey coloured phases at the interfaces of the dark grey (α-Ti) phases. This characteristic microstructure was observed throughout the entire alloy (Fig. 6). According to the Ti-Cu binary phase diagram, the β-Ti phase exhibits a eutectoid transformation at 790 °C with 7.1 wt.% Cu [36]. During cooling from this region, precipitation of Ti_2Cu from the β-Ti phase takes place and α-Ti + Ti_2Cu phases are formed. In an alloy such as 9 wt.% Cu, where hypereutectoid transformation occurs, the Ti_2Cu phase precipitates in

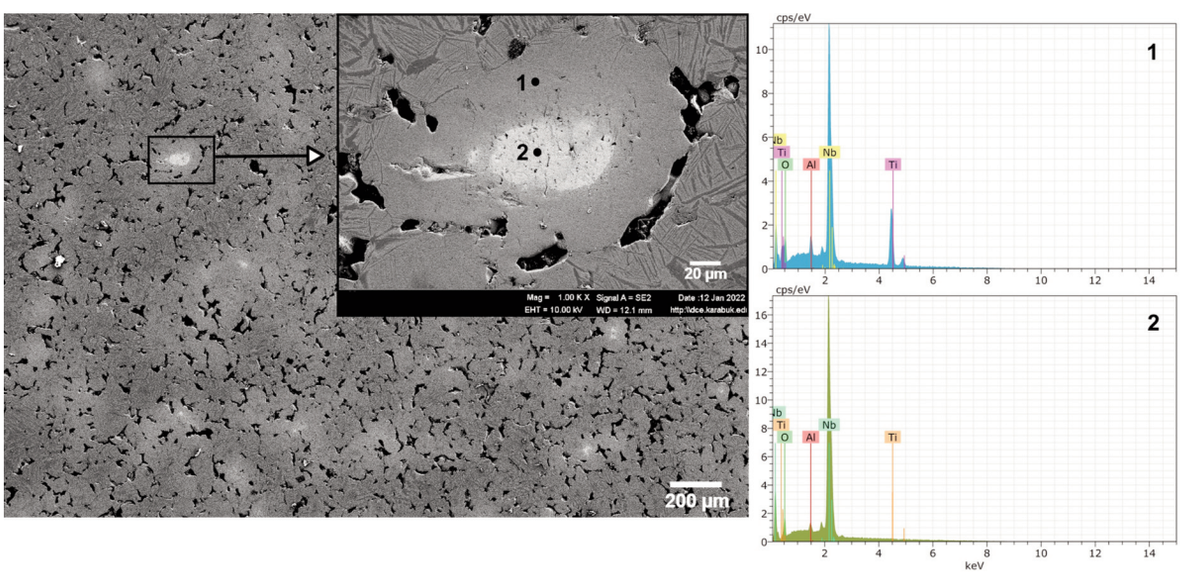

Figure 3. *Microstructural image of the Ti-18Nb alloy and EDS spectra of indicated points*

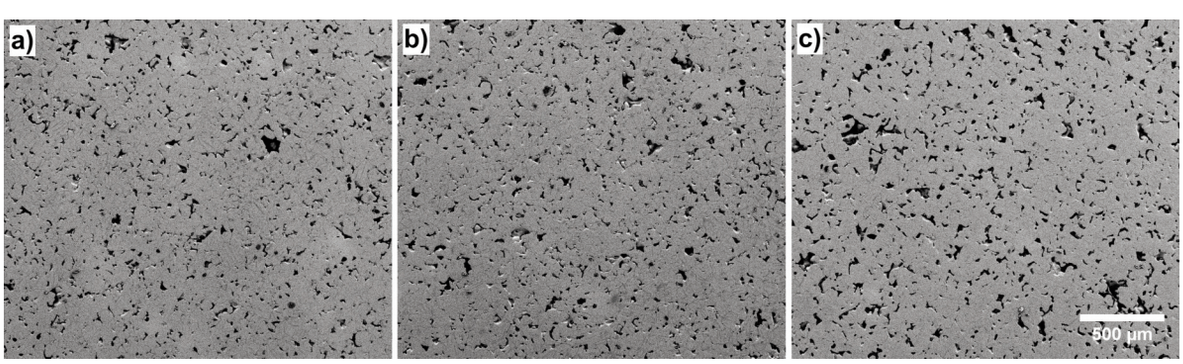

Figure 4. *Low-magnification SEM images of the samples: a) Ti-18Nb-5Cu, b) Ti-18Nb-7Cu, and (c) Ti-18Nb-9Cu*

β-Ti upon solidification, and the β-Ti phase transforms into Ti_2Cu and α-Ti phases below the eutectoid line [36, 42].

EDS analysis of the microstructure indicated that phases labelled 4 and 8 correspond to the β-Ti phase, whereas the remaining lath-like dark areas represent the α-Ti phase. Analysis of points 1, 3 and 7 taken from the ash-grey regions formed in the microstructure of the alloy with 9 wt.% Cu addition, reveals only the Cu and Nb-rich parts of the α-Ti phase. Line EDS analysis of the designated area showed a progressive increase in Nb content within this ash-grey region, which formed subsequently to α-Ti, and a higher Cu concentration compared to the β-Ti phase. During solidification of alloys with an α+β+Ti_2Cu microstructure, the Nb-rich β phase initially forms. As the crystal grows, regions farther from the grain centre contain a higher concentration of Cu. As a result, Cu concentration increases towards the β-Ti grain boundaries, and the Ti_2Cu phases precipitate [29]. This formation is not clearly observed in the other alloys. The analysis also indicated that the α-Ti phase contains more Cu than β-Ti. Previous studies have reported that the α-Ti phase can contain more Cu than the β-Ti phase, suggesting that Cu can thermally diffuse into α-Ti, forming a solid solution [26].

The addition of Cu had a noticeable effect on both the microstructure and mechanical properties of the Ti-18Nb alloy. Fig. 7 shows a representative compression test curve and average compression test results for each alloy. In addition, Table 2 provides the mechanical values of the samples. The standard deviations of the values measured from mechanical

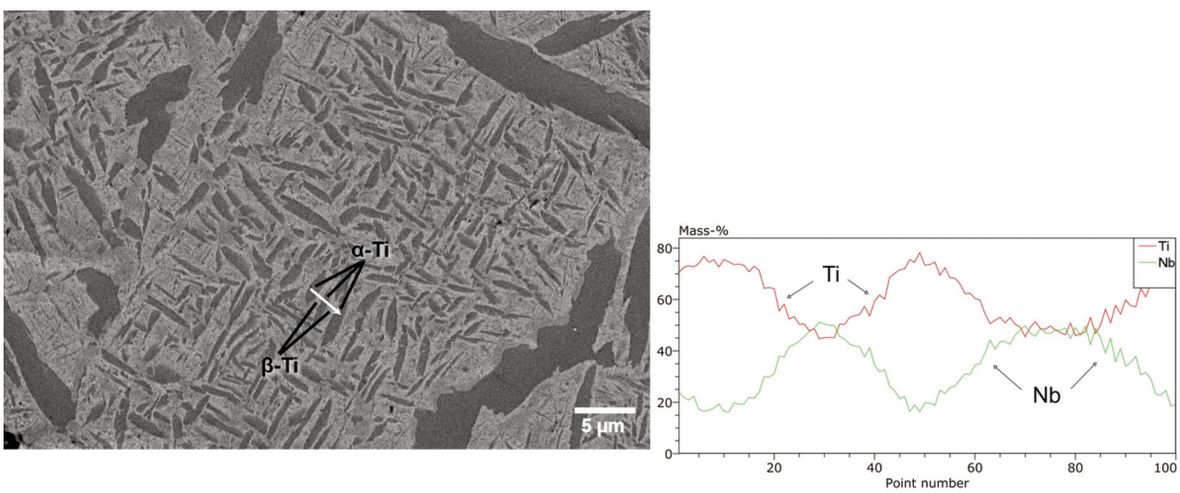

Figure 5. *Microstructural image and line EDS profile of the Ti-18Nb-7Cu alloy*

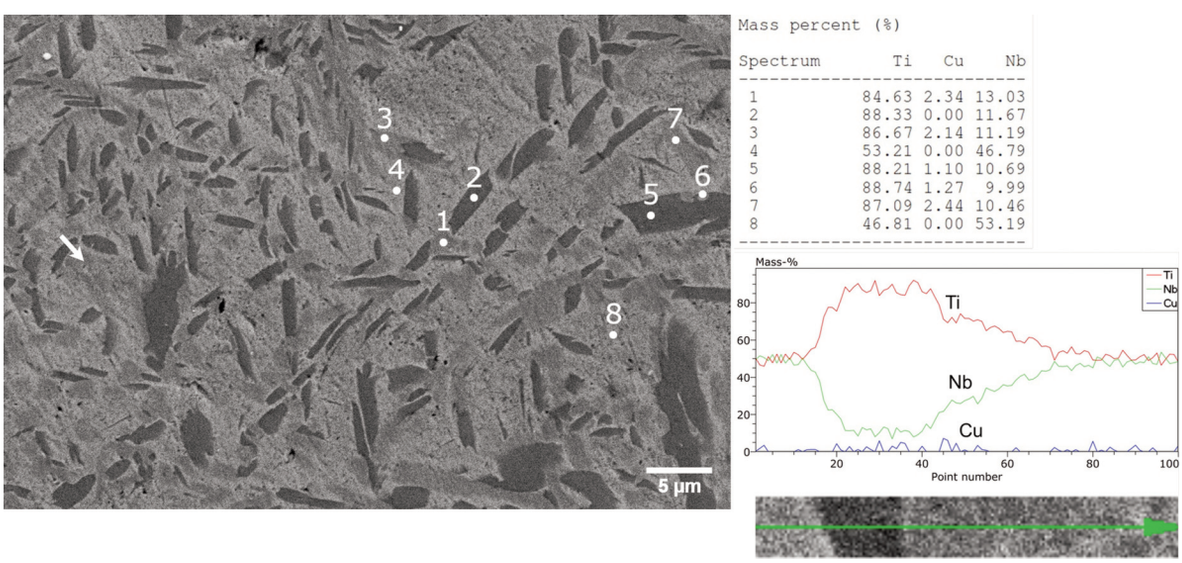

Figure 6. *Microstructural image with point and line EDS analyses of the Ti-18Nb-7Cu*

tests (Table 2) were determined to be below 10%.

The average compression test results in Fig. 7b and Table 2 show that the yield strength of the Ti-18Nb alloy increases almost linearly with the addition of Cu. In contrast, the compressive strength increased slightly with 5 wt.% Cu, followed by a considerable increase at 7 wt.% Cu, and a further, albeit slight, enhancement with 9 wt.% Cu. Previous research investigating Cu additions to titanium at various concentrations (2, 5, 7, and 10 wt.%) reported that the Ti-7Cu alloy achieved the highest compressive strength [26]. Similarly, the compressive strength of the alloys demonstrated a substantial increase with the addition of 7 wt.% Cu. However, further Cu addition resulted in only a minor or no further increase in compressive strength.

A trend consistent with that observed for compressive strength was noted in the hardness measurements (Table 2). The 7 wt.% Cu-containing alloy exhibited the highest hardness, which remained relatively constant or slightly decreased with increasing Cu amount. The observed increase in hardness was achieved by solid solution strengthening in the α-Ti phase and precipitation of the Ti_2Cu phase [43]. Given the presence of comparable phases in the Ti-18Nb-xCu alloys, it is suggested that a similar mechanism underlies their increased hardness. A consistent pattern was noted between Vickers and Brinell macro-hardness readings, although Brinell hardness values were marginally lower, likely due to inherent manufacturing imperfections.

Analysis of the elastic modulus in response to increasing Cu content revealed an initial slight rise with 5 wt.% Cu, followed by a subsequent decrease with further Cu addition. Yuan et al. [44] reported that the compressive and yield strength increased when 4, 7, 10 and 13 wt.% Cu were added to the Ti-13Nb-13Zr alloy. Their findings indicated that the elastic modulus initially declined with increasing copper, and subsequently increased, with their 7 wt.% Cu alloys exhibiting the lowest modulus. In the present investigation, a similar trend was observed with Cu addition in our alloy, which also featured α and β-Ti phases, confirming that the 7 wt.% Cu alloy exhibited the minimum elastic modulus.

Considering that bulk (arc-melted) Ti-15Nb alloy has an elastic modulus of 77 GPa and Ti-7Cu has an elastic modulus of 108 GPa [26, 33], it becomes evident that the elastic modulus is primarily governed by production parameters and the intrinsic porosity of the material. However, compact human cortical bone exhibits an elastic modulus ranging from 12–17 GPa, which can drop to as low as 3 GPa in areas like cancellous bone [45, 46]. Therefore, the alloys developed in this study demonstrate suitable elastic modulus values, effectively contributing to the reduction of stress shielding.

Biomedical implant materials are typically

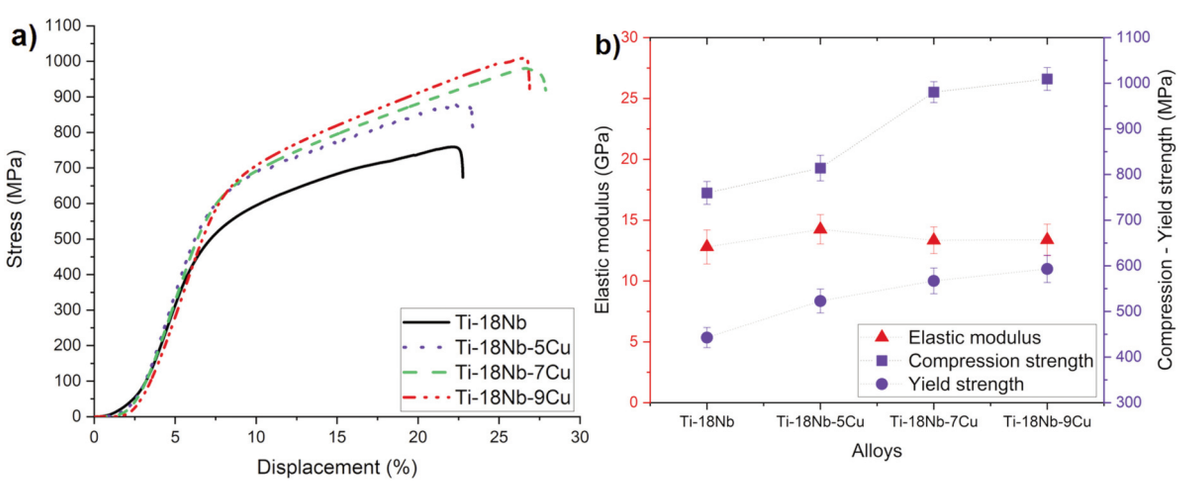

Figure 7. *a) An example compression test curve and b) determined average values*

Table 2. *The average mechanical values of samples*

Samples	*E (GPa)*	σ_{max}*(MPa)*	σ_y*(MPa)*	U_r (MJ/m^3)	HV	HB
Ti-18Nb	1280	759.61	442.68	7.65	150±25	110±6
Ti-18Nb-5Cu	14.24	814.1	522.87	9.6	197±21	132±5
Ti-18Nb-7Cu	13.34	980.49	566.9	12.04	222± 24	140±1
Ti-18Nb-9Cu	13.38	1009.2	593.08	13.15	216±28	138±3

engineered to undergo elastic deformation during their functional lifespan. Hence, the material's capacity to absorb energy (resilience) during elastic deformation is of considerable importance. The modulus of resilience (U_r), represented by the area beneath the elastic deformation curve on a stress-strain diagram, can be quantified using the following equation [47]:

$$U_r = \sigma_y^2 / 2E \quad (1)$$

In the formula, E is the modulus of elasticity, and σ_y is the yield strength. The formula demonstrates that the combination of high yield strength and low modulus of elasticity will lead to a higher resilience value, which is expected to be advantageous in biomaterial applications.

The lowest modulus of resilience (U_r) among the produced alloys was observed in the Ti-18Nb alloy, with a value of 7.65 MJ/m³. and consistently increased with Cu addition: 9.60 MJ/m³ for Ti-18Nb-5Cu, 12.04 MJ/m³ for Ti-18Nb-7Cu, and 13.15 MJ/m³ for Ti-18Nb-9Cu. This trend indicates that Cu addition enhances the material's ability to absorb elastic energy before yielding. For comparison, the modulus of resilience is typically reported in the range of 1–5 MJ/m³ for many conventional titanium alloys [48], with a value of 3.7 MJ/m³ for the widely used Ti-6Al-4V (TAV) alloy [49]. In contrast, higher values, such as 22.56 MJ/m³, have been reported for β-phase dominant alloys like Ti-10Mo-1.25Si-10Zr [48]. The relatively high Ur values observed in the present study, especially with Cu addition, highlight the improved elastic energy absorption capacity of the developed Ti-18Nb-xCu alloys.

4. Conclusions

This study investigated the effect of Cu addition on the sintering behavior, microstructure, and mechanical properties of Ti-18Nb alloy produced by the conventional powder metallurgy process. The main findings are as follows:

- A homogeneous microstructure was achieved for Ti-18Nb alloys with 5 wt.% Cu and higher content after sintering at 1150°C for 5 hours, whereas these conditions were insufficient for the base Ti-18Nb alloy. Cu addition facilitated the dissolution of Nb particles and promoted a more homogeneous structure by lowering the melting point of the Ti-Cu phase, thereby positively influencing the sintering process.

- Volumetric porosity in Cu-containing alloys decreased by approximately 5% compared to the Ti-18Nb alloy.

- XRD analysis confirmed the presence of Ti_2Cu, alpha (α) and beta (β) Ti phases in all Cu-containing alloys, with the intensity of Ti_2Cu peaks increasing with higher Cu content. Cu addition also supported the formation of the beta phase.

- Hardness values increased with Cu addition, the highest hardness (222 HV or 140 HB) was measured in the 7 wt.% Cu alloy.

- Yield strength showed an almost linear increase with rising Cu content. Compressive strength notably increased with 7 wt.% Cu addition (reaching 980 MPa) and slightly exceeded this value with 9 wt.% Cu.

- Elastic modulus initially increased with 5 wt.% Cu addition, subsequently declining with 7 and 9 wt.% Cu. The Ti-18Nb-7Cu alloy exhibited the lowest elastic modulus (13.34 GPa) among Cu-containing alloys.

- The combination of high yield strength and low elastic modulus resulted in high resilience (12.04 MJ/m³) for the Ti-18Nb-7Cu alloy.

The Ti-18Nb-7Cu alloy exhibits superior mechanical properties, including high compressive (980 MPa) and yield (567 MPa) strengths, peak hardness (222 HV), and the lowest elastic modulus (13.34 GPa), making it a promising candidate for biomedical implant applications.

Acknowledgements

This work was supported by the Scientific Research Projects Coordination Unit of Karabuk University [grant number KBÜBAP-22-YL-048]. This article was derived from the master's thesis of Muhamad Saad Faaik titled "Investigation the Mechanical Properties of Porous Ti-18Nb-XCu Alloys for Biomedical Applications".

Authors contribution

Huseyin Demirtas: conceptualization, methodology, formal analysis, writing, review and editing, Rana Afif Anaee: methodology, formal analysis, review and editing, Muhamad Saad Faaik: conceptualization, methodology, formal analysis.

Data availability

The datasets generated and analysed during the current study are available from the corresponding author on reasonable request.

Conflict of interest

The authors declare no conflict of interest.

References

[1] S. Pervaiz, A. Rashid, I. Deiab, M. Nicolescu, Influence of tool materials on machinability of titanium- and nickel-based alloys: A review, Materials and Manufacturing Processes, 29 (3) (2014) 219–252. https://doi.org/10.1080/10426914.2014.880460

[2] M. Niinomi, Recent research and development in titanium alloys for biomedical applications and healthcare goods, Science and Technology of Advanced Materials, 4 (5) (2003) 445. https://doi.org/10.1016/j.stam.2003.09.002

[3] Y. Li, C. Wong, J. Xiong, P. Hodgson, C. Wen, Cytotoxicity of titanium and titanium alloying elements, Journal of Dental Research, 89 (5) (2010) 493–497.
https://doi.org/10.1177/0022034510363675

[4] M.T. Mohammed, Z.A. Khan, M. Geetha, Effect of thermo-mechanical processing on microstructure and electrochemical behavior of Ti–Nb–Zr–V new metastable β titanium biomedical alloy, Transactions of the Nonferrous Metals Society of China, 25 (3) (2015) 759–769.
https://doi.org/10.1016/S1003-6326(15)63661-5

[5] L. Zhang, K. Wang, L. Xu, S. Xiao, Y. Chen, Effect of Nb addition on microstructure, mechanical properties and castability of β-type Ti–Mo alloys, Transactions of the Nonferrous Metals Society of China, 25 (7) (2015) 2214–2220.
https://doi.org/10.1016/S1003-6326(15)63834-1

[6] M. Fellah, N. Hezil, M. Abdul Samad, R. Djellabi, A. Montagne, A. Mejias, S. Kossman, A. Iost, A. Purnama, A. Obrosov, S. Weiss, Effect of molybdenum content on structural, mechanical, and tribological properties of hot isostatically pressed β-Type titanium alloys for orthopedic applications, Journal of Materials Engineering and Performance, 28 (10) (2019) 5988–5999.
https://doi.org/10.1007/s11665-019-04348-w

[7] X. Zhao, M. Niinomi, M. Nakai, J. Hieda, Beta type Ti–Mo alloys with changeable Young's modulus for spinal fixation applications, Acta Biomaterialia, 8 (5) (2012) 1990–1997. https://doi.org/10.1016/j.actbio.2012.02.004

[8] C. Zhao, X. Zhang, P. Cao, Mechanical and electrochemical characterization of Ti–12Mo–5Zr alloy for biomedical application, Journal of Alloys and Compounds, 509 (32) (2011) 8235–8238. https://doi.org/10.1016/j.jallcom.2011.05.090

[9] M. Fellah, N. Hezil, M. A. Hussein, M. Abdul Samad, M.Z. Touhami, A. Montagne, A. Iost, A. Obrosov, S. Weiss, Preliminary investigation on the bio-tribocorrosion behavior of porous nanostructured β-type titanium based biomedical alloys, Materials Letters, 257 (2019) 126755. https://doi.org/https://doi.org/10.1016/j.matlet.2019.126755

[10] Y.W. Chai, H.Y. Kim, H. Hosoda, S. Miyazaki, Self-accommodation in Ti–Nb shape memory alloys, Acta Materialia, 57 (14) (2009) 4054–4064. https://doi.org/10.1016/j.actamat.2009.04.051

[11] L. Xu, S. Xiao, J. Tian, Y. Chen, Y. Huang, Microstructure and dry wear properties of Ti-Nb alloys for dental prostheses, Transactions of the Nonferrous Metals Society of China, 19 (2009) 639–644. https://doi.org/10.1016/S1003-6326(10)60124-0

[12] Y. Tomio, T. Furuhara, T. Maki, Effect of cooling rate on superelasticity and microstructure evolution in Ti-10V-2Fe-3Al and Ti-10V-2Fe-3Al-0.2 N alloys, Materials Transactions, 30 (12) (2009) 2731–2736. https://doi.org/10.2320/matertrans.ma200909

[13] T. Maeshima, M. Nishida, Shape memory properties of biomedical Ti-Mo-Ag and Ti-Mo-Sn alloys, Materials Transactions, 45 (4) (2004) 1096–1100. https://doi.org/10.2320/matertrans.45.1096

[14] E. Eisenbarth, D. Velten, M. Müller, R. Thull, J. Breme, Biocompatibility of β-stabilizing elements of titanium alloys, Biomaterials, 25 (26) (2004) 5705–5713. https://doi.org/10.1016/j.biomaterials.2004.01.021

[15] M. Geetha, A.K. Singh, R. Asokamani, A.K. Gogia, Ti based biomaterials, the ultimate choice for orthopaedic implants–a review, Progress in Materials Science, 54 (3) (2009) 397–425. https://doi.org/10.1016/j.pmatsci.2008.06.004

[16] J.-Y. Rho, T.Y. Tsui, G.M. Pharr, Elastic properties of human cortical and trabecular lamellar bone measured by nanoindentation, Biomaterials, 18 (20) (1997) 1325–1330.
https://doi.org/10.1016/S0142-9612(97)00073-2

[17] M. Niinomi, Y. Liu, M. Nakai, H. Liu, H. Li, Biomedical titanium alloys with Young's moduli close to that of cortical bone, Regenerative Biomaterials, 3 (3) (2016) 173–185.
https://doi.org/10.1093/rb/rbw016

[18] H. Demirtas, The effect of porosity on the mechanical properties of Ti–8Nb–8Zr–8Cu alloy, Materials Science and Technology, 38 (14) (2022) 1118–1126. https://doi.org/10.1080/02670836.2022.2081447

[19] S. Gündüz, D. Taştemür, An investigation of plastic deformation behaviour of Nb-V microalloyed steel produced by powder metallurgy, Journal of Mining and Metallurgy, Section B: Metallurgy, 60 (3) (2024) 305–315.
https://doi.org/10.2298/JMMB231226025T

[20] J. Xiong, Y. Li, X. Wang, P. Hodgson, C. Wen, Mechanical properties and bioactive surface modification via alkali-heat treatment of a porous Ti–18Nb–4Sn alloy for biomedical applications, Acta Biomaterialia, 4 (6) (2008) 1963–1968. https://doi.org/10.1016/j.actbio.2008.04.022

[21] G. Ryan, A. Pandit, D. Apatsidis, Fabrication methods of porous metals for use in orthopaedic applications, Biomaterials, 27 (13) (2006) 2651–2670. https://doi.org/10.1016/j.biomaterials.2005.12.002

[22] B.V. Krishna, S. Bose, A. Bandyopadhyay, Low stiffness porous Ti structures for load-bearing implants, Acta Biomaterialia, 3 (6) (2007) 997–1006. https://doi.org/10.1016/j.actbio.2007.03.008

[23] G. Grass, C. Rensing, M. Solioz, Metallic copper as an antimicrobial surface, Applied and Environmental Microbiology, 77 (5) (2011) 1541–1547. https://doi.org/10.1128/AEM.02766-10

[24] Nowak, J. Szade, E. Talik, M. Zubko, D. Wasilkowski, M. Dulski, K. Balin, A. Mrozik, J. Peszke, Physicochemical and antibacterial characterization of ionocity Ag/Cu powder nanoparticles, Materials Characterization, 117 (2016) 9–16. https://doi.org/10.1016/j.matchar.2016.04.013

[25] E. Zhang, F. Li, H. Wang, J. Liu, C. Wang, M. Li, K. Yang, A new antibacterial titanium–copper sintered

alloy: Preparation and antibacterial property, Materials Science and Engineering C, 33 (7) (2013) 4280–4287. https://doi.org/10.1016/j.msec.2013.06.016

[26] C. Yi, Z. Ke, L. Zhang, J. Tan, Y. Jiang, Z. He, Antibacterial Ti-Cu alloy with enhanced mechanical properties as implant applications, Materials Research Express, 7 (10) (2020) 105404. https://doi.org/10.1088/2053-1591/abc371

[27] H. Demirtaş, M. Riyadh, R. Anaee, Wear and corrosion properties for the effect of addition Cu to Ti–18Nb biomaterial, Chemistry Africa, 6 (6) (2023) 3185–3193.

https://doi.org/10.1007/s42250-023-00690-8

[28] H.R.H. Hraam, S. Islak, A.M.M. Gariba, Microstructure and mechanical properties of Ti-Cu-based materials produced by using reactive melt infiltration and liquid phase sintering techniques, Metallography, Microstructure, and Analysis, 12 (4) (2023) 662–671.

https://doi.org/10.1007/s13632-023-00978-8

[29] K. Sato, M. Takahashi, Y. Takada, Construction of Ti-Nb-Ti2Cu pseudo-ternary phase diagram, Dental Materials Journal, 39 (3) (2020) 422–428. https://doi.org/10.4012/dmj.2018-394

[30] Y. Xu, J. Jiang, Z. Yang, Q. Zhao, Y. Chen, Y. Zhao, The effect of copper content on the mechanical and tribological properties of hypo-, hyper- and eutectoid Ti-Cu alloys, Materials, 13 (15) (2020) 3411. https://doi.org/10.3390/ma13153411

[31] R. Elkilani, Ç. Harun, H. Abushrenta, O. Albahlol, M.A. ERDEN, B. Cicek, Effects of hot rolling on microstructures, wear and corrosion resistance of Mo-Ni-W P/M alloyed steels, Journal of Mining and Metallurgy, Section B: Metallurgy, 60 (3) (2024) 367–380.

https://doi.org/10.2298/JMMB240404030E

[32] H. Li, T. Lei, J. Zhao, Q. Shang, Z. Lin, Production of Ti–13Nb–13Zr alloy by powder metallurgy (P/M) via sintering hydrides, Materials and Manufacturing Processes, 31 (6) (2016) 719–724. https://doi.org/10.1080/10426914.2014.994775

[33] M. Fellah, N. Hezil, M.Z. Touhami, A. Obrosov, S. Weiß, E.B. Kashkarov, A.M. Lider, A. Montagne, A. Iost, Enhanced structural and tribological performance of nanostructured Ti–15Nb alloy for biomedical applications, Results in Physics, 15 (2019) 102767. https://doi.org/10.1016/j.rinp.2019.102767

[34] L.J. Gibson, M.F. Ashby, Cellular Solids: Structure and Properties, 2nd Edition, Cambridge University Press, Cambridge, 1997

[35] P.A. Benavides, B. Soto, R.H. Palma, Liquid phase sintering of mechanically alloyed Mo-Cu powders, Materials Science and Engineering: A, 701 (2017) 237–244.

https://doi.org/10.1016/j.msea.2017.06.090

[36] J.L. Murray, The Cu−Ti (Copper-Titanium) system, Bulletin of Alloy Phase Diagrams, 4 (1) (1983) 81–95. https://doi.org/10.1007/BF02880329

[37] V.A.R. Henriques, C.A.A. Cairo, C.R.M. Silva, J.C. Bressiani, Microstructural evolution of Ti-13Nb-13Zr alloy during sintering, Materials Science Forum, 498 (2005) 40–48. https://doi.org/10.4028/www.scientific.net/MSF.498-499.40

[38] G.V. Martins, C.R.M. Silva, C.A. Nunes, V.A.R. Henriques, L.A. Borges, J.P.B. Machado, Microstructural evolution of Ti-10NB and Ti-15NB alloys produced by the blended elemental technique, Materials Science Forum, 660 (2010) 152–157. https://doi.org/10.4028/www.scientific.net/MSF.660-661.152

[39] D. Zhao, K. Chang, T. Ebel, H. Nie, R. Willumeit, F. Pyczak, Sintering behavior and mechanical properties of a metal injection molded Ti–Nb binary alloy as biomaterial, Journal of Alloys and Compounds, 640 (2015) 393–400. https://doi.org/10.1016/j.jallcom.2015.04.039

[40] Q.Y. Sun, Z.T. Yu, R.H. Zhu, Dynamic fracture toughness of Ti–2.5Cu alloy strengthened with nano-scale particles at room and low temperatures, Materials Science and Engineering A, 483–484 (2008) 131–134. https://doi.org/10.1016/j.msea.2006.11.171

[41] Shi, D. Cai, J. Hu, X. Zhao, G. Qin, Y. Han, E. Zhang, Development of a low elastic modulus and antibacterial Ti-13Nb-13Zr-5Cu titanium alloy by microstructure controlling, Materials Science and Engineering C, 126 (2021) 112116. https://doi.org/10.1016/j.msec.2021.112116

[42] M.R. Akbarpour, H.M. Mirabad, A. Hemmati, H.S. Kim, Processing and microstructure of Ti-Cu binary alloys: A comprehensive review, Progress in Materials Science, 127 (2022) 100933. https://doi.org/10.1016/j.pmatsci.2022.100933

[43] M. Kikuchi, Y. Takada, S. Kiyosue, M. Yoda, M. Woldu, Z. Cai, O. Okuno, T. Okabe, Mechanical properties and microstructures of cast Ti–Cu alloys, Dental Materials, 19 (3) (2003) 174–181. https://doi.org/10.1016/S0109-5641(02)00027-1

[44] Y. Yuan, Z. Ke, L. Zhang, Y. Jiang, Z. He, Mechanical, corrosion and antibacterial properties of Ti-13Nb-13Zr-based alloys with various Cu contents, Materials Research Express, 8 (11) (2021) 115403. https://doi.org/10.1088/2053-1591/ac2f74

[45] T. Hanawa, Research and development of metals for medical devices based on clinical needs, Science and Technology of Advanced Materials, 13 (6) (2012) 064102. https://doi.org/10.1088/1468-6996/13/6/064102

[46] M. Niinomi, M. Nakai, Titanium-based biomaterials for preventing stress shielding between implant devices and bone, International Journal of Biomaterials, 2011 (2011) 1–10.

https://doi.org/10.1155/2011/836587

[47] W.D. Callister, Materials Science and Engineering: An Introduction, 7th Edition, John Wiley & Sons, New York, 2007

[48] Y. Zhan, C. Li, W. Jiang, β-type Ti-10Mo-1.25Si-xZr biomaterials for applications in hard tissue replacements, Materials Science and Engineering C, 32 (6) (2012) 1664–1668. https://doi.org/10.1016/j.msec.2012.04.059

[49] J. Coakley, K.M. Rahman, V.A. Vorontsov, M. Ohnuma, D. Dye, Effect of precipitation on mechanical properties in the β-Ti alloy Ti–24Nb–4Zr–8Sn, Materials Science and Engineering A, 655 (2016) 399–407.

https://doi.org/10.1016/j.msea.2015.12.024

UTICAJ SADRŽAJA Cu NA MIKROSTRUKTURU I MEHANIČKA SVOJSTVA Ti-18Nb-XCu LEGURE PROIZVEDENE METALURGIJOM PRAHA

Huseyin Demirtas [a, *], Rana Afif Anaee [b], Muhamad Saad Faaik [a]

[a] Univerzitet Karabuk, Katedra za mašinske i metalne tehnologije, Karabuk, Turska
[b] Tehnološki univerzitet, Katedra za inženjerstvo materijala, Bagdad, Irak

Apstrakt

Ovo istraživanje je ispitivalo uticaj različitih koncentracija bakra (Cu) (0, 5, 7 i 9 mas.%) na ponašanje pri sinterovanju, razvoj mikrostrukture i mehaničke karakteristike Ti-18Nb legure, proizvedene konvencionalnom metalurgijom praha. Pod specifičnim uslovima sinterovanja (1150 °C tokom 5 sati), dodatak Cu je doveo do homogenije mikrostrukture i podstakao potpuno rastvaranje čestica Nb. Analiza rendgenskom difrakcijom (XRD) potvrdila je prisustvo alfa (α) i beta (β) Ti faza, kao i Ti_2Cu faze, čiji se intenzitet pika povećavao sa porastom sadržaja Cu. Mehanička svojstva su značajno poboljšana dodatkom Cu. Granica tečenja se povećavala gotovo linearno sa sadržajem Cu. Pritisna čvrstoća se značajno povećala sa 7 mas.% Cu, dostižući 980 MPa, i neznatno je premašila ovu vrednost sa 9 mas.% Cu. Vrednosti tvrdoće su se povećale usled rastvornog ojačavanja α-Ti faze i precipitacije Ti_2Cu faze, pri čemu je najveća tvrdoća (222 HV) uočena kod legure sa 7 mas.% Cu. Modul elastičnosti se u početku povećavao sa 5 mas.% Cu, a zatim se naknadno smanjivao sa daljim dodavanjem Cu; Ti-18Nb-7Cu legura je pokazala najniži modul elastičnosti od 13,34 GPa. Pored toga, energija elastične deformacije legura se poboljšala formiranjem Ti_2Cu faze, a postignuta je maksimalna vrednost od 13, 15 MJ m^{-3}.

Ključne reči: *Ti legura; Biomaterijal; Metalurgija praha; Test kompresije; Modul elastičnosti; Energija elastične deformacije*